

Modules in the Photoreceptor RGS9-1-G_{β5L} GTPase-accelerating Protein Complex Control Effector Coupling, GTPase Acceleration, Protein Folding, and Stability*

Received for publication, August 2, 2000, and in revised form, August 31, 2000
Published, JBC Papers in Press, September 7, 2000, DOI 10.1074/jbc.M006982200

Wei He‡, Lisha Lu‡, Xue Zhang‡, Heithem M. El-Hodiri§, Ching-Kang Chen¶||, Kevin C. Slep**, Melvin I. Simon¶, Milan Jamrich§, and Theodore G. Wensel‡ ‡‡

From the ‡Verna and Marrs McLean Department of Biochemistry and Molecular Biology and the §Department of Molecular and Cellular Biology, Baylor College of Medicine, Houston, Texas 77030, the ¶Division of Biology, 147-75, California Institute of Technology, Pasadena, California 91125, and the **Department of Molecular Biophysics and Biochemistry, Yale University, New Haven, Connecticut 06511

RGS (regulators of G protein signaling) proteins regulate G protein signaling by accelerating GTP hydrolysis, but little is known about regulation of GTPase-accelerating protein (GAP) activities or roles of domains and subunits outside the catalytic cores. RGS9-1 is the GAP required for rapid recovery of light responses in vertebrate photoreceptors and the only mammalian RGS protein with a defined physiological function. It belongs to an RGS subfamily whose members have multiple domains, including G_γ-like domains that bind G_{β5} proteins. Members of this subfamily play important roles in neuronal signaling. Within the GAP complex organized around the RGS domain of RGS9-1, we have identified a functional role for the G_γ-like-G_{β5L} complex in regulation of GAP activity by an effector subunit, cGMP phosphodiesterase γ and in protein folding and stability of RGS9-1. The C-terminal domain of RGS9-1 also plays a major role in conferring effector stimulation. The sequence of the RGS domain determines whether the sign of the effector effect will be positive or negative. These roles were observed *in vitro* using full-length proteins or fragments for RGS9-1, RGS7, G_{β5S}, and G_{β5L}. The dependence of RGS9-1 on G_{β5} co-expression for folding, stability, and function has been confirmed *in vivo* using transgenic *Xenopus laevis*. These results reveal how multiple domains and regulatory polypeptides work together to fine tune G_{tα} inactivation.

Most pathways for transducing signals from the cell surface to amplified second messenger cascades within cells of animals are organized around G proteins. Sufficient information is now available from the genomes of nematodes and humans to conclude that heptahelical transmembrane proteins of the G protein-coupled class constitute by far the largest class of receptors in these animals. The burden of communicating complex signals from this enormous variety of receptors must be borne

by the relatively small number (on the order of 20) of distinct G protein α subunits (G_α) found in these genomes. It is hard to imagine such a scheme operating successfully unless the G proteins are helped in their task of encoding this information by additional regulatory proteins. Indeed, a family of proteins, comparable in size to the G_α family, have been found to be capable of exerting such regulation on activated G_α; these are the RGS (regulators of G protein signaling) family of GTPase-accelerating proteins (GAPs)¹ (1, 2).

Among vertebrate RGS proteins, one whose physiological role in G protein signaling is particularly clear is the photoreceptor-specific isoform RGS9-1. Removal of RGS9-1 by immunodepletion (3) or gene inactivation (4) leads to loss of GTPase acceleration for the phototransduction G protein transducin (G_t), and without this GTPase acceleration, mouse rods have dramatically slowed photoresponses. The catalytic core of RGS9-1 is sufficient to accelerate GTP hydrolysis by G_t (5–7), but there is clear evidence that RGS9-1 does not act alone in accelerating GTP hydrolysis. The PDE γ subunit of the photoreceptor effector enzyme cGMP phosphodiesterase (PDE6) has been known for some time to enhance GTPase acceleration (8), and it is now established that it works by increasing the activity of RGS9-1 (3, 4). Rods of mice with a form of PDE γ deficient in RGS9-1 enhancement also have slowed photoresponse recovery (9). PDE γ is able to exert its GAP-enhancing effect on the RGS9 catalytic core, but the effect is much weaker than observed for endogenous RGS9-1 (6, 7, 10), implying that other domains and/or subunits play a role in coupling GAP enhancement to this effector subunit.

In addition to PDE γ , the photoreceptor-specific G_β isoform G_{β5L} has also been implicated in RGS9-1 function. RGS9-1 is extracted from rod outer segments as a complex with G_{β5L} (11), and RGS9-1 knockout mice are completely lacking G_{β5L}. The closely related short isoform G_{β5S} greatly enhances the activity of the striatal isoform RGS9–2 in an oocyte expression system coupled to muscarinic regulation of potassium channels (12). RGS6 and RGS7 have been isolated as complexes with G_{β5S} (13, 14), and it has been proposed that members of the RGS9 subfamily of RGS proteins (RGS6, RGS7, RGS9, and RGS11 in mammals; EGL-10 and EAT-16 in *Caenorhabditis elegans*, dRGS7 in *Drosophila*) all bind G_{β5} isoforms through their G protein γ -like (GGL) domains (15). However, the role, if any, of G_{β5S} and G_{β5L} in regulation of GAP activity remains uncertain,

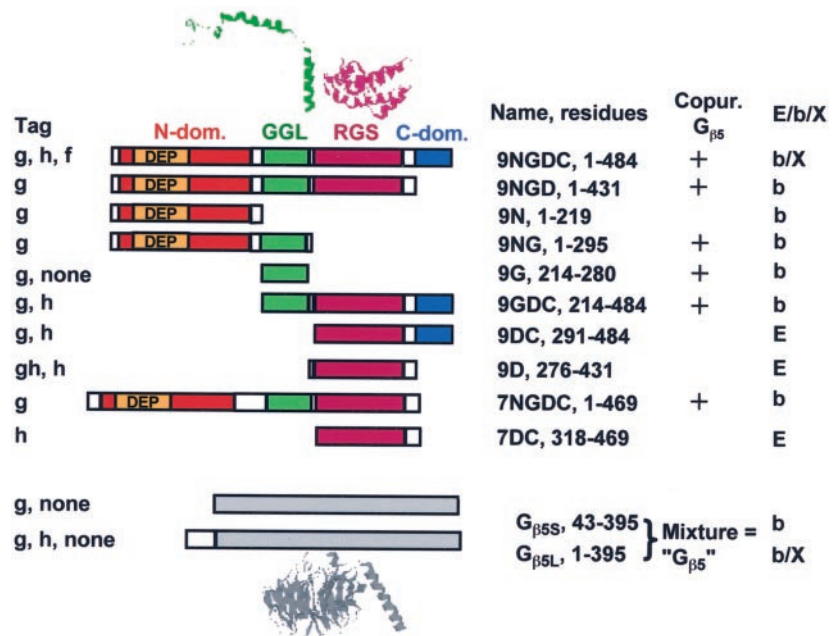
* This work was supported by grants from the National Institutes of Health and by the Robert A. Welch Foundation. The costs of publication of this article were defrayed in part by the payment of page charges. This article must therefore be hereby marked "advertisement" in accordance with 18 U.S.C. Section 1734 solely to indicate this fact.

¶ Present address, Dept. of Ophthalmology, Eccles Institute of Human Genetics, University of Utah, Salt Lake City, UT 84112.

‡‡ To whom correspondence should be addressed: Verna and Marrs McLean Dept. of Biochemistry and Molecular Biology, Baylor College of Medicine, Houston, TX 77030. Tel.: 713-798-6994; Fax: 713-796-9438; E-mail: twensel@bcm.tmc.edu.

¹ The abbreviations used are: GAP, GTPase-accelerating protein; PDE, cGMP phosphodiesterase (PDE6); GGL, G protein γ -like; PCR, polymerase chain reaction; GST, glutathione S-transferase; EGFP, enhanced green fluorescent protein.

FIG. 1. Protein constructs used to dissect roles of protein modules in RGS9-1, RGS7, and $G_{\beta 5}$. Major domains are coded by position and color as indicated, with linker regions in white. *N-dom.* refers to the N-terminal domain (including DEP domain) of RGS9-1. *C-dom.* refers to the C-terminal domain of RGS9-1. *Tag* refers to N-terminal fusions: GST (*g*), His₆ (*h*), both (*gh*), EGFP (*f*), and none (*none*). *Name* refers to identifiers used in text with tag label (*e.g.* *gh*) as prefix (no prefix for no tag), *e.g.* *g9GDC* refers to a construct with the GGL domain, RGS domain, and C-terminal domain of RGS9-1, fused to an N-terminal GST tag. *Copur.* $G_{\beta 5}$ indicates whether the proteins were purified as a complex with co-expressed $G_{\beta 5}$. *E/b/X* refers to expression system: *E* for *E. coli*, *b* for baculovirus, and *X* for *X. laevis*. $G_{\beta 5}$ refers to the mixture of $G_{\beta 5S}$ and $G_{\beta 5L}$ produced in Sf9 cells by use of alternative translation initiation sites.



as one report (16) described blocking by $G_{\beta 5S}$ of G_{α} binding to RGS7, whereas another described GAP activity of an RGS- $G_{\beta 5}$ complex (17), and oocyte expression experiments suggest that $G_{\beta 5S}$ actually enhances GAP activity (12).

Regulation of activity by domains and subunits outside the catalytic RGS domains appears to be the rule rather than the exception for the RGS family (18–20). They contain multiple domains with known (*e.g.* PDZ domains) or unknown (*e.g.* DEP (dishevelled/EGL-10/pleckstrin homology) domains) functions. RGS9-1 contains an N-terminal domain (including a DEP domain) of unknown function, the GGL domain, and the catalytic RGS core domain. These are shared by the other members of the RGS9 subfamily. In addition, RGS9-1 contains a unique C-terminal domain, produced partly by the alternative RNA processing, which distinguishes RGS9-1 from the striatal isoform RGS9–2 (21, 22). The experiments described here establish roles for different domains and for $G_{\beta 5L}$ in regulation of GAP activity and effector coupling and in protein folding and stability.

EXPERIMENTAL PROCEDURES

Buffers—Compositions were as follows. GAPN buffer, 10 mM Tris, pH 7.4, 100 mM NaCl, 2 mM MgCl₂, 1 mM dithiothreitol; and lysis buffer, 50 mM Tris, pH 8.0, 500 mM NaCl, 1 mM dithiothreitol, 1% Nonidet P-40.

Constructs—The DNA fragments of bovine RGS9-1 encoding residues 1–484 (9NGDC), 1–219 (9N), 214–280 (9G), 214–484 (9GDC), and 291–484 (9DC), the DNA fragment of bovine RGS7 encoding residues 1–469 (7NGDC), the DNA fragment of murine RGS7 encoding residues 318–469 (7DC), and the DNA fragment of murine $G_{\beta 5L}$ encoding residues 1–395 were amplified from the corresponding cDNAs by PCR using cloned *Pfu* DNA polymerase (Stratagene). The initial codons of these fragments were replaced by *Nde*I restriction sites, and *Bam*HI restriction sites were inserted at their 3' ends. These fragments were then cloned in frame into *Nde*I/*Bam*HI sites of pET14b (Novagen) or modified pGEX-2TK (23) vector to express N-terminal His₆-tagged or GST-tagged proteins in *Escherichia coli*. These fragments with N-terminal His₆ or GST tags were subsequently cloned into pVL1392 (PharMingen) to generate recombinant baculoviruses for expression in Sf9 cells. The fragment from bovine RGS9 encoding residues 1–295 (9NG) was digested by *Nde*I/*Eco*47 III from the fragment of RGS9 encoding residues 1–484, cloned into pAS2 (CLONTECH) to obtain a *Bam*HI site to the 3' end, and then cloned into pVL1392. The mouse $G_{\beta 5L}$ cDNA was excised using *Eco*RI/*Xba*I digestion from the plasmid, pcDNAI-amp- $G_{\beta 5L}$ (24), and then cloned into pVL1392 to generate recombinant baculoviruses for expression of untagged $G_{\beta 5L}$ proteins in

Sf9 cells. The fragment from bovine RGS9 encoding residues 276–431 (9D) was amplified by PCR. *Bam*HI and *Eco*RI restriction sites were inserted at its 5' end and 3' end, respectively. Then this *Bam*HI/*Eco*RI fragment was subcloned into *Bgl*II/*Eco*RI sites of a modified pGEX-2T plasmid, which has a polylinker, *Bam*HI-His₆-*Bgl*II, appending to its *Bam*HI site. pVL1392-g9GD (residues 214–431) and pVL1392-g9NGD (residues 1–431) were made by removing the RGS9-C domain from pVL1392-g9GDC and pVL1392-g9NGDC. The *Nco*I/*Bam*HI RGS9 fragments in pVL1392-g9GDC and pVL1392-g9NGDC were replaced by the *Nco*I/*Eco*RI RGS9 fragment of pGEX-9D. The *Bam*HI end of the vector and *Eco*RI end of the RGS9 fragment were filled with Klenow large fragment before ligation.

The pXOP-EGFP-RGS9-1 and pXOP- $G_{\beta 5L}$ expressing plasmids were constructed as follows. The pXOP-C₁-EGFP vector (a kind gift from Dr. Barry Knox, SUNY Upstate Medical University, Syracuse) was cut by *Age*I and *Apa*LI to collect the 1.7-kilobase fragment including a 1.4-kilobase *Xenopus* rhodopsin promoter sequence. The promoter sequence was then ligated to the *Age*I/*Apa*LI pEGFP-C₂ backbone to produce pXOP-C₂-EGFP. A bovine RGS9-1 cDNA *Eco*RI/*Bam*HI fragment was subcloned in frame into *Eco*RI/*Bam*HI sites of pXOP-C₂-EGFP to generate pXOP-EGFP-RGS9-1 expression plasmid. To construct pXOP- $G_{\beta 5L}$, a *Eco*RI/*Sac*II $G_{\beta 5L}$ cDNA fragment was subcloned in frame into *Eco*RI/*Sac*II sites of pXOP-C₂-EGFP to generate pXOP-EGFP- $G_{\beta 5L}$. Then the EGFP sequence was removed by digestion of *Age*I/*Bgl*II. The sticky ends were filled with Klenow large fragment and religated to generate pXOP- $G_{\beta 5L}$ expression plasmid.

Expression and Purification of Recombinant Proteins—Recombinant baculoviruses were isolated following cotransfection of the linearized BaculoGold viral DNA (PharMingen) and the transfer vector into Sf9 cells according to the manufacturer's instructions. Untagged $G_{\beta 5S}$ baculovirus is a generous gift from Dr. James Garrison, University of Virginia (25). Cells were grown as monolayers in 150-mm culture dishes in Insect-Xpress medium (Bio Whittaker) supplemented with 8% fetal bovine serum and 10 μ g/ml gentamicin and infected with recombinant viruses at 80% confluency and harvested 48 h later. Cell pellets were suspended to a density of 2.5×10^7 cells/ml in lysis buffer and protease inhibitors (0.03 mg/ml leupeptin, 0.017 mg/ml pepstatin A, 0.005 mg/ml aprotinin, 0.03 mg/ml lima bean trypsin inhibitor, and solid phenylmethylsulfonyl fluoride) for 30 min at 4 °C. Cell lysates were sonicated and then clarified by centrifugation at $20,000 \times g$ for 30 min at 4 °C. The supernatants were applied to glutathione-Sepharose 4B resin (Amersham Pharmacia Biotech) or nickel-nitrilotriacetic acid resin (Qiagen) depending on the tag used. For His₆-tagged proteins, 20 mM imidazole was added to the supernatant to reduce nonspecific binding to the resin. The resin was washed with lysis buffer and GAPN buffer plus 20 mM imidazole, and His₆-tagged protein was eluted with 250 mM imidazole in GAPN buffer. For GST-tagged proteins, the resin was washed with GAPN buffer, and the protein was eluted with 40 mM glutathione in

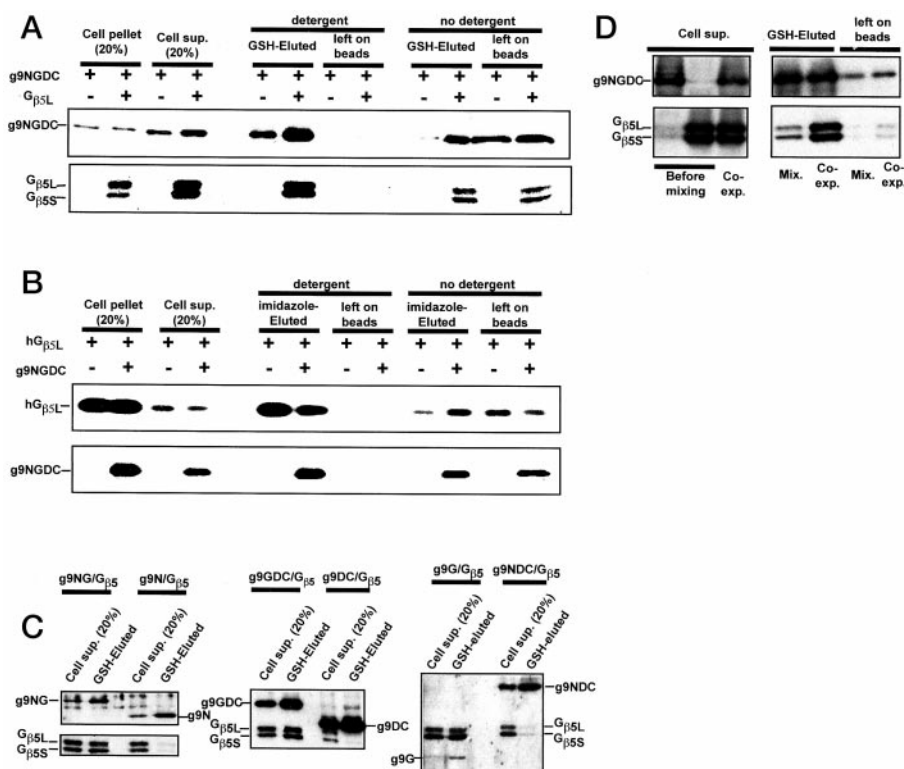


FIG. 2. RGS9-1 and $G_{\beta 5}$ solubility depends on heterodimer formation. GST-tagged proteins were expressed in Sf9 cells and then extracted with detergent (wherever present, detergent was 1% Nonidet P-40). Samples of the cell pellets and supernatants (*Cell sup.*) after detergent extraction were used for immunoblot analysis, and the remaining supernatants were loaded onto glutathione beads. After washing, proteins were eluted in GSH buffer with or without detergent as indicated in A and B and with detergent in C and D. In all panels, RGS9-1 and $G_{\beta 5}$ were detected on immunoblots by anti-RGS9-1c antiserum and anti- $G_{\beta 5}$ antiserum except that g9N in C was detected by anti-RGS9-N antiserum. A, GST-tagged RGS9-1 (g9NGDC) was effectively eluted in soluble form without detergent only when co-expressed with $G_{\beta 5}$ and purified as a complex. g9NGDC was expressed in Sf9 cells with or without co-expression of $G_{\beta 5}$ and then purified by GSH affinity column. B, His₆-tagged $G_{\beta 5L}$ (h $G_{\beta 5L}$) was effectively eluted in soluble form as a complex with GST-tagged RGS9-1 (g9NGDC) without detergent. h $G_{\beta 5L}$ was expressed in Sf9 cells with or without co-expression of g9NGDC and then purified by immobilized Ni²⁺ affinity chromatography. C, the GGL domain of RGS9-1 was necessary and sufficient for the binding of $G_{\beta 5}$. GST-tagged RGS9-1 fragments were co-expressed with $G_{\beta 5}$ in Sf9 cells, and affinity purified using detergent in the GSH elution buffer. D, efficient formation and stability of the g9NGDC- $G_{\beta 5}$ complex in Sf9 cells required co-expression. g9NGDC was affinity purified either from the mixed extracts of cells separately infected by g9NGDC and $G_{\beta 5}$ baculoviruses (*Mix.*) or from the extracts of cells simultaneously infected by g9NGDC and $G_{\beta 5}$ baculoviruses (*Co-exp.*).

GAPN buffer. The purified proteins were stored in -20°C in 40% glycerol. For $G_{\beta 5}$ expression, we routinely used a virus encoding untagged $G_{\beta 5L}$ and found that both long ($\sim 60\%$) and short ($\sim 40\%$) forms were consistently produced and co-purified with RGS9-1. Because the short form reacts with monospecific antibodies to a common epitope in $G_{\beta 5S}$ and $G_{\beta 5L}$ (see Fig. 2), has identical mobility to $G_{\beta 5S}$ produced by a different virus (see Fig. 4A), and is not observed when a $G_{\beta 5L}$ expression construct differing in its ribosome binding site and in the presence of an N-terminal His₆ fusion peptide is used (see Fig. 4A), we conclude that the short form is likely $G_{\beta 5S}$ formed by alternative translation initiation at the second ATG in the coding sequence.

Recombinant proteins were also expressed in *E. coli* using BL21(DE3)pLysS cells and standard procedures. g9DC and h9DC were expressed in insoluble form, so they were solubilized from inclusion bodies using 6 M guanidinium chloride. g9DC was renatured by step dialysis before purification. h9DC was first allowed to bind to nickel-nitrilotriacetic acid resin under denaturing conditions and then renatured on the resins according to the manufacturer's (Qiagen) instructions. h9D was generated from the thrombin cleavage of purified gh9D following the standard protocol and then purified by nickel-nitrilotriacetic acid resin.

Single Turnover GTPase Assay—Single turnover G_{ta} GTPase assays were carried out as described with or without exogenous PDE γ (26). Briefly, urea washed rod outer segments were mixed with purified transducin, various amount of recombinant RGS proteins and PDE γ in GAPN buffer. Then GTP hydrolysis was initiated by adding 7 μl of [γ -³²P]GTP (Amersham Pharmacia Biotech) to 14 μl of the above mixture by vortexing. The reaction was quenched by 100 μl of 5% trichloroacetic acid at various times, and P_i released from hydrolyzed GTP was determined by activated charcoal assay. Final concentrations were: 15

μM rhodopsin, 1 μM transducin, and 0 or 2 μM recombinant His₆-PDE γ . The first order rate constant for GTP hydrolysis (k_{inact}) was obtained by fitting data to single exponentials.

Antibodies and Western Blot Analysis—Polyclonal anti-RGS9-1c and polyclonal anti- $G_{\beta 5}$ antisera were generated as described (6, 24). Polyclonal anti-RGS9-N rabbit antisera were raised (Bethyl Labs) against recombinant bovine h9N protein. Western blot analyses were performed as described (6). The following dilutions of primary antibodies were used: 1:1000 dilution of polyclonal anti-RGS9-1c antiserum, 1:500 dilution of polyclonal anti-RGS9-N antiserum, and 1:500 dilution of polyclonal anti- $G_{\beta 5}$ antiserum.

Transgenesis—For transgenesis, DNA was purified using the Qiagen midi-prep protocol, and pXOP-EGFP-RGS9-1 was digested with *RsrII* and pXOP- $G_{\beta 5L}$ with *ApaLI*. The linearized plasmids were purified after digestion (Qiaex II, Qiagen), with final elution in water. Transgenic *Xenopus laevis* embryos were prepared by restriction enzyme-mediated integration as described (27) except that the amounts of restriction enzyme used (*NotI*) and egg extract were reduced to 0.15 units and 2 μl /transgenesis reaction, respectively. Restriction enzyme-mediated integration was carried out in $0.4\times$ MMR (28) containing 6% (w/v) Ficoll. $1\times$ MMR contains 100 mM NaCl, 2 mM KCl, 1 mM MgCl₂, 2 mM CaCl₂, 5 mM HEPES, pH 7.4. Embryos were transferred to $0.1\times$ MMR, 6% Ficoll at the 4–8 cell stage. Properly gastrulating embryos were raised in $0.1\times$ MMR until approximately stage 42 (29) and then transferred to dechlorinated water. Tadpoles were anesthetized in 0.01% 3-aminobenzoic acid ethyl ester (Sigma) and monitored for green fluorescent protein expression using an Olympus fluorescent dissecting microscope. To extract genomic DNA, tadpoles were sacrificed and incubated over night at 55°C in 50 mM Tris, pH 8.0, 50 mM EDTA, 0.5% SDS and 100 $\mu\text{g/ml}$ proteinase K (Life Technologies, Inc.). After phenol-

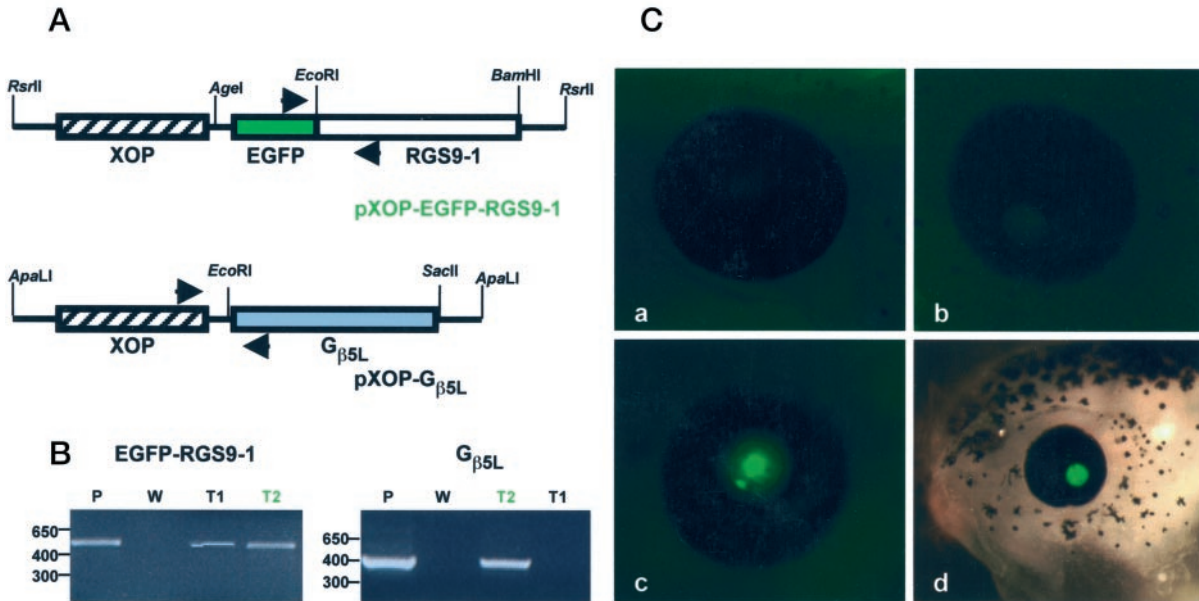


FIG. 3. Expression of EGFP-RGS9-1 in transgenic *Xenopus* tadpoles requires $G_{\beta 5L}$. *A*, maps of transgene constructs pXOP-EGFP-RGS9-1 and pXOP- $G_{\beta 5L}$. On the map lines, the 1.4-kilobase rhodopsin promoter sequences are shown as hatched boxes, EGFP coding sequences are shown as a solid green box, coding sequences for RGS9-1 are shown as open boxes, and coding sequences for $G_{\beta 5L}$ are shown as a light blue box. Arrows represent the primers for PCR genotyping. *B*, genomic DNA purified from 1 month old tadpole with EGFP retinal-expression phenotype (T2), tadpole without EGFP phenotype (T1), and control wild type tadpole (W) were analyzed by PCR to detect the integration of XOP-EGFP-RGS9-1 (left panel) and XOP- $G_{\beta 5L}$ (right panel). For each analysis, transgene constructs (P) were used as positive control. The predicted size for PCR products of RGS9-1 and $G_{\beta 5L}$ transgenes are 500 and 383 base pairs, respectively. *C*, green fluorescent protein fluorescence in an eye of a wild type tadpole (panel *a*), a transgenic tadpole with XOP-EGFP-RGS9-1 (panel *b*), and a transgenic tadpole with both XOP-EGFP-RGS9-1 and XOP- $G_{\beta 5L}$ (panel *c*). The bright green fluorescent protein fluorescence was only observed from the tadpole bearing both EGFP-RGS9-1 and $G_{\beta 5L}$. Panel *d*, lateral view of another transgenic tadpole with both EGFP-RGS9-1 and $G_{\beta 5L}$ transgenes. The picture is a combination of a bright field image and a fluorescence field image.

chloroform extraction, DNA was precipitated by adding 2 volumes of 100% ethanol. The DNA pellets were washed in 1 ml of 70% ethanol, dried by speed vacuum, and resuspended in TE. About 0.4 μ g of genomic DNA was used as template in PCR reactions.

RESULTS

Dependence on Heterodimer Formation of RGS9-1 and $G_{\beta 5}$ Solubility—To dissect the roles of individual protein modules in the RGS9-1- $G_{\beta 5}$ complex, we expressed and purified a number of protein fragments and complexes (Fig. 1). Full-length RGS9-1 is readily expressed at high levels in either bacterial (6) or baculovirus (Fig. 2) systems but is produced almost entirely in an insoluble form (data not shown). In the detergent Nonidet P-40, RGS9-1 and $G_{\beta 5}$ can be extracted from insect cells into solution for affinity purification. We observed a striking difference between the behavior of RGS9-1 with and without $G_{\beta 5}$: RGS9-1 is eluted from the affinity matrix in soluble form without detergent when bound to $G_{\beta 5}$ (Figs. 2, A and B, and 4A) but in the absence of $G_{\beta 5}$ can only be eluted when detergent is added. Moreover, once purified, RGS9-1 without $G_{\beta 5}$ precipitates when Nonidet P-40 is removed, whether by dilution or slow dialysis. It precipitates even when Nonidet P-40 is exchanged for either of two detergents shown previously to solubilize the RGS9-1- $G_{\beta 5L}$ complex from photoreceptor membranes in active form, octyl glucoside (3) or lauryl sucrose (11) (data not shown). $G_{\beta 5L}$ also displayed a dependence on RGS9-1 for solubility, but it was less stringent. Some h $G_{\beta 5L}$ could be recovered in soluble form without RGS9-1, but the amount was significantly reduced (Fig. 2B).

RGS9-1 Binds $G_{\beta 5}$ through the $G\gamma$ -like Domain—The formation of the RGS9-1- $G_{\beta 5}$ complex is clearly mediated through the GGL domain of RGS9-1. All GST-tagged fragments containing the GGL domain co-purified with co-expressed $G_{\beta 5}$ (Fig. 2C), including a GST-GGL construct (g9G), whereas constructs containing either the RGS9-1 domains N-terminal to the GGL

domain (g9N) or those C-terminal to the GGL domain (g9DC) or both (g9NDC) did not bind co-expressed $G_{\beta 5}$. RGS7, which also contains a GGL domain, also co-purified with $G_{\beta 5}$ (see Fig. 4A).

Efficient formation and stability of the RGS9-1- $G_{\beta 5}$ complex required co-expression (Fig. 2D). When cells were simultaneously infected with viruses expressing RGS9-1 and $G_{\beta 5}$, the complex was readily co-purified. In contrast, when extracts of cells separately infected with the two different virus preparations were mixed, very little of the complex formed as revealed by the much lower amount of $G_{\beta 5}$ co-purifying with RGS9-1. Thus, $G_{\beta 5}$ is required during or immediately after translation for efficient formation of the RGS9-1- $G_{\beta 5}$ complex.

Co-expression of $G_{\beta 5}$ Is Required for RGS9-1 Expression in Vivo—Further evidence for a dependence on $G_{\beta 5}$ for production of functional RGS9-1 was provided *in vivo* by transgenesis experiments in *X. laevis*. In five trials in which a construct directing expression of a EGFP-RGS9-1 fusion (f9NGDC; Fig. 3A) was used for fertilization without a $G_{\beta 5L}$ construct, none of the surviving tadpoles displayed detectable EGFP signal in their eyes. Genotyping of 19 revealed that 11 had the transgene inserted in their genomes. In four trials in which f9NGDC and $G_{\beta 5L}$ constructs were co-injected, at least one tadpole with detectable retinal EGFP signal (Fig. 3C) was obtained every time. Genotyping of five animals with integrated f9NGDC construct and detectable retinal EGFP signal revealed that the $G_{\beta 5L}$ construct was also integrated in all (Fig. 3B). No animals expressing detectable levels of EGFP-RGS9-1 have been found to date that do not have the $G_{\beta 5L}$ construct integrated, although two tadpoles containing integrated EGFP-RGS9-1 but not $G_{\beta 5L}$ were found among the tadpoles without detectable signal from one co-injection trial. In all these trials we have not found a single animal that has both f9NGDC and $G_{\beta 5L}$ constructs integrated but that displays no retinal EGFP signal.

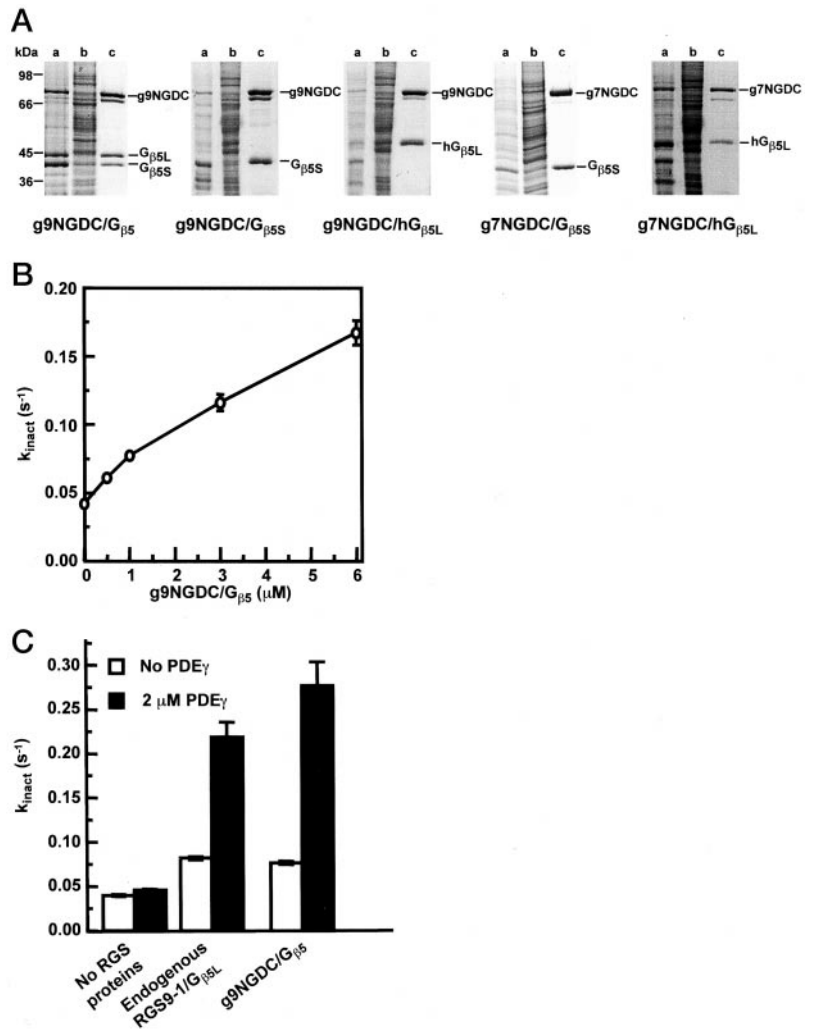


FIG. 4. The GAP activity of the complex of GST-tagged RGS9-1 (g9NGDC) and G β_5 . *A*, purification of g9NGDC·G β_5 , g9NGDC·G β_{5S} , g9NGDC·hG β_{5L} , g7NGDC·G β_{5S} , and g7NGDC·hG β_{5L} complexes. g9NGDC and G β_5 , g9NGDC and G β_{5S} , g9NGDC and hG β_{5L} , g7NGDC and G β_{5S} , or g7NGDC and hG β_{5L} were coexpressed in Sf9 cells and then purified by GSH affinity column. No detergent was present in the elution buffer. Pellets of cell lysates (*lanes a*), supernatants of cell lysates (*lanes b*; 10% relative to *lanes a*), and the purified complexes (*lanes c*; g9NGDC·G β_5 , 0.6 μ g; g9NGDC·G β_{5S} , 1.0 μ g; g9NGDC·hG β_{5L} , 1.0 μ g; g7NGDC·G β_{5S} , 1.5 μ g; g7NGDC·hG β_{5L} , 1.0 μ g) were separated on SDS-PAGE and stained by Coomassie Blue. *B*, concentration dependence of the GAP activity of g9NGDC·G β_5 without PDE γ . *C*, PDE γ enhancement of GAP activity of endogenous RGS9-1·G β_{5L} (9NGDC·G β_{5L}) complex and g9NGDC·G β_5 complex (1 μ M). Endogenous RGS9-1·G β_{5L} was supplied as isotonic washed rod outer segment membranes at a final R α concentration of 15 μ M. Single turnover GTPase assays of G α were carried out as described under "Experimental Procedures."

Thus, just as G β_{5L} protein expression in murine photoreceptor cells requires the presence of RGS9-1 (4), RGS9-1 expression (or at least, detectable overexpression of our construct) in *Xenopus* photoreceptors requires the presence of G β_{5L} .

GAP Activity and Effector Regulation of RGS9-1·G β_5 Complex—Once sufficient amounts of the RGS9-1·G β_5 complex had been purified from infected SF9 cells (Fig. 4A), we were able to check it for catalytic activity. It has been previously suggested (30) that the rod outer segment GAP, or the RGS9-1·G β_{5L} complex, has no GAP activity in the absence of PDE γ . As shown in Fig. 4B, just as rod outer segment membranes exhaustively washed to remove PDE show significant GAP activity toward G α (31), recombinant RGS9-1·G β_5 significantly accelerates GTP hydrolysis by G α in the absence of any subunits of PDE. Thus, the GAP activity of this complex does not have an absolute requirement for PDE γ . However, PDE γ does enhance its GAP activity greatly. As shown in Fig. 4C, the enhancement is very similar to that observed for the endogenous GAP in rod outer segment membranes, in marked contrast to previous observations for the core RGS domain (5–7, 10). As with other RGS proteins, the core RGS domain of RGS9-1 is sufficient to accelerate GTP hydrolysis by G α . However, enhancement of the GAP activity of the RGS domain of RGS9 by PDE γ is very modest. Thus, the additional protein modules in the RGS9-1·G β_5 complex must contribute most of the interactions required for regulation by PDE γ .

All Domains of RGS9-1 Contribute to Regulation of GAP Activity and Effector Coupling—The constructs described in Fig. 1 allowed us to assess the relative contributions of different protein modules in the RGS9-1·G β_5 complex to GAP activity with and without PDE γ (Fig. 5). Interestingly, when assayed at 6 μ M, in the presence of PDE γ , the GAP activities of all constructs in Fig. 5 (A–D) were similar, with none differing from any other by more than a factor of two. The most striking differences were observed in the absence of PDE γ . GAP preparations containing the GGL domain·G β_5 complex (Fig. 5, A and D) had lower basal GAP activity than those containing only the RGS core domain or the RGS domain plus the C-terminal domain (Fig. 5, B and C), especially at concentrations above 1 μ M. Comparison of the results from different proteins assayed in Fig. 5 suggests that the GGL domain·G β_5 complex confers most of the effector sensitivity and does so primarily by inhibition of GAP activity in the absence of PDE γ . Because the complex containing only the short form of G β_5 (g9NGDC·G β_{5S} ; Fig. 5A) had identical activity to that of the complex containing a mixture of G β_5 isoforms (g9NGDC·G β_5) with about 60% G β_{5L} , the additional 42 amino acid residues on the long isoform do not play an important role in regulating GAP activity or PDE γ enhancement.

The N-terminal domain, containing the DEP module, also seems to play a role through a modest enhancement of PDE γ -stimulated GAP activity as revealed by comparison of Fig. 5 (A

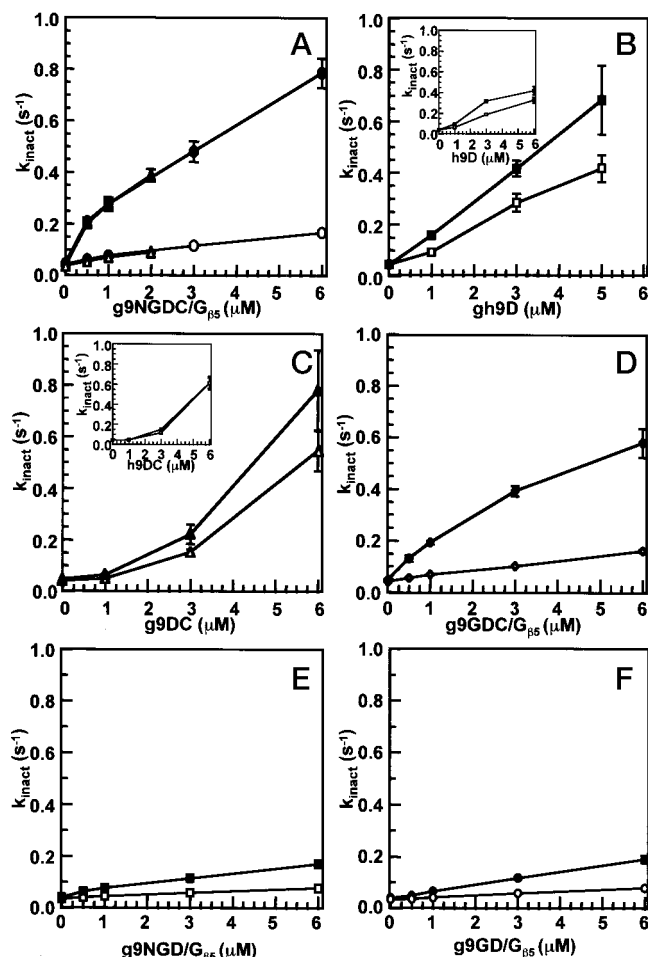


FIG. 5. Contribution of protein modules to the basal GAP activity and effector regulation. Single turnover assays of G_{tox} GTPase with (filled symbols) or without (open symbols) PDE γ . Concentration dependence of the GAP activity was as follows: A, g9NGDC- $G_{\beta 5}$ (circles) and g9NGDC- $G_{\beta 5S}$ (triangles); B, gh9D (inset, h9D); C, g9DC (inset, h9DC); D, g9GDC- $G_{\beta 5}$; E, g9NGD- $G_{\beta 5}$; F, g9GD- $G_{\beta 5}$.

and D). We also compared h9NGDC- $G_{\beta 5}$ to g9NGDC- $G_{\beta 5}$ and found little difference (<11%) in basal or PDE γ -stimulated GAP activities for the different N-terminal fusions (data not shown), consistent with a noncritical role for the N-terminal domain of RGS9.

The C-terminal domain of RGS9-1 also plays an important role but only in the context of a complex containing the covalently attached GGL- $G_{\beta 5}$ couple. Complexes of $G_{\beta 5}$ with both g9NGD (Fig. 5E) and g9GD (Fig. 5F) showed low basal GAP activity, as observed for the corresponding complexes containing the C-terminal domain (g9NGDC, Fig. 5A; g9GDC, Fig. 5D), indicating that covalently attached GGL- $G_{\beta 5}$ is sufficient to inhibit the GAP activity of the RGS core domain. However, PDE γ only weakly countered the inhibition of GAP activity conferred by GGL- $G_{\beta 5}$ in the absence of the C-terminal domain, strongly suggesting that the C-terminal domain is required to work cooperatively with PDE γ to relieve inhibition by GGL- $G_{\beta 5}$. In the absence of GGL- $G_{\beta 5}$, the effect of removing the C-terminal domain is less dramatic. The g9DC construct displays an anomalous cooperative behavior (Fig. 5C) not seen with the other constructs (although there is a hint of such behavior for gh9D; Fig. 5B). This apparent cooperativity is not due to the well known GST dimerization equilibrium as it is also clearly seen in the His $_6$ -tagged construct h9DC (Fig. 5C,

inset). Given this behavior, it is hard to attribute much significance to the small differences in PDE γ enhancement seen in comparing Figs. 5 (B and C). Thus, the C-terminal domain must interact directly or indirectly with the GGL- $G_{\beta 5}$ module to explain the differences between the results shown in Fig. 5 (E and F) as compared with those in 5B and 5C. In separate studies,² we have found that the C-terminal domain of RGS9-1 is important for tethering RGS9-1 to membranes, possibly providing an additional indirect role for this domain in effector coupling by localizing the RGS9-1- $G_{\beta 5L}$ complex on the disc membranes where PDE resides.

GGL Domain Containing $G_{\beta 5}$ Complexes Acts as Functional Modules without Attached RGS Domain—We also explored whether the $G_{\beta 5}$ -GGL domain complex could influence activity of the RGS domain when they were not covalently attached. The two complexes tested, g $G_{\beta 5L}$ -9G and g9NG- $G_{\beta 5}$, had no influence on GTP hydrolysis of G_{tox} without the RGS domain in the absence or presence of PDE γ , nor did they affect GAP activity of a complex (h9GDC- $G_{\beta 5}$) containing the GGL domain covalently attached to the RGS domain (Fig. 6). However, they strongly influenced the GAP activity of the RGS domain in either h9D or h9DC (Fig. 6). They mimicked the covalently attached GGL domain complexed to $G_{\beta 5}$ in enhancing the GAP stimulation by PDE γ but surprisingly stimulated, rather than inhibited, GAP activity in the absence of PDE γ . These results suggest a model (Fig. 6C) in which PDE γ induces a change from an inhibitory conformation imposed by the covalent attachment of the NG- $G_{\beta 5}$ modules to a catalysis-promoting conformation that is also available when NG- $G_{\beta 5}$ is not constrained by covalent attachment but is still stabilized by PDE γ in that case.

The RGS Domain Determines whether PDE γ Enhances or Inhibits GAP Activity—Finally, to assess the specificity of these interactions, we compared RGS9-1 and the closely related neuronal RGS protein, RGS7 (Fig. 7). Like g9NGDC- $G_{\beta 5}$, g7NGDC- $G_{\beta 5}$ displays GAP activity in the absence of PDE γ , but in sharp contrast to RGS9-1, this RGS7 complex is not stimulated but rather inhibited by PDE γ (Fig. 7A). The PDE γ inhibition was still observed even when $G_{\beta 5S}$ was replaced by h $G_{\beta 5L}$ (Fig. 4A) for formation of the complex with RGS7 (data not shown), indicating that the PDE γ inhibition is intrinsic to RGS7 and not a result of its binding to $G_{\beta 5S}$ rather than to $G_{\beta 5L}$.

The effects of g9NG- $G_{\beta 5}$ on the RGS domain of RGS7 (h7DC) are similar to its effects on RGS9-1 (h9DC); basal GAP activity is enhanced, and modulation of activity by PDE γ is enhanced. The striking difference is that as observed for all RGS proteins tested so far besides RGS9-1, the effect of PDE γ is inhibition, rather than stimulation, of GAP activity (Fig. 7B). Taken together with previous studies (5, 10), these results support the conclusion that although GGL- $G_{\beta 5}$ and perhaps the N-terminal domain are important in determining the basal activity and the extent of PDE γ modulation, the sign of the modulation (negative or positive) is determined by key residues within the RGS domain.

DISCUSSION

Three major conclusions emerge from the work described here: 1) RGS9-1 and $G_{\beta 5L}$ act as an obligate heterodimer. The function and even the production and maintenance of each depends upon the other. This mutual dependence is observed at the levels of GAP activity, solubility, and conformational stability of the recombinant proteins *in vitro* and at the level of protein expression *in vivo*. 2) $G_{\beta 5L}$ confers tight regulation by the effector subunit PDE γ on the catalytic RGS domain. It

² W. He and T. G. Wensel, unpublished observations.

FIG. 6. The N-terminal RGS9 domain and GGL-G_{β5} complex both contribute to effector dependence, even without covalent linkage to catalytic domain. Single turnover assays of G_{τα} GTPase with and without PDE_γ. *A*, addition of g9NG-G_{β5} significantly enhances the GAP activity of h9DC, whereas it has no effect on h9GDC-G_{β5}. g9NG-G_{β5} itself has no detectable GAP activity. *B*, addition of gG_{β5L}-9G significantly enhances the GAP activity of h9DC. gG_{β5L}-9G itself has no detectable GAP activity. *C*, schematic model for the modulation of the GAP activity of the RGS core domain by modules within the RGS9-1-G_{β5L} complex. The expected secondary structure of the RGS domain is suggested by use of the RGS4 structure (37), and those of G_{τα}, the GGL domain, and G_{β5L} by use of the G_{τα}-GDP, G_{τγ}, and G_{τβ} structures, respectively, from the transducin heterotrimer structure (38). Positions and shapes of modules are intended as purely schematic representations.

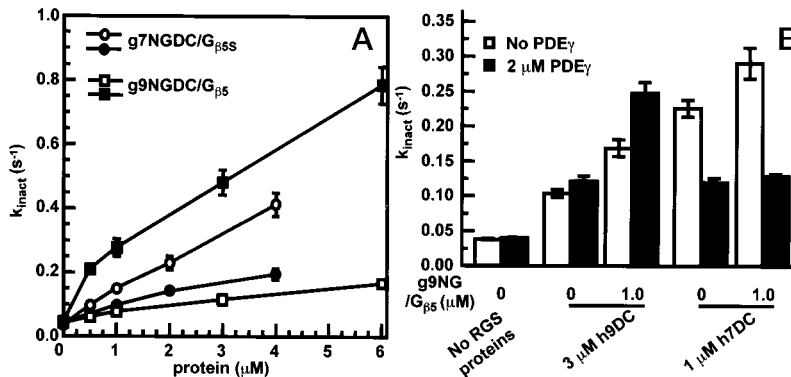
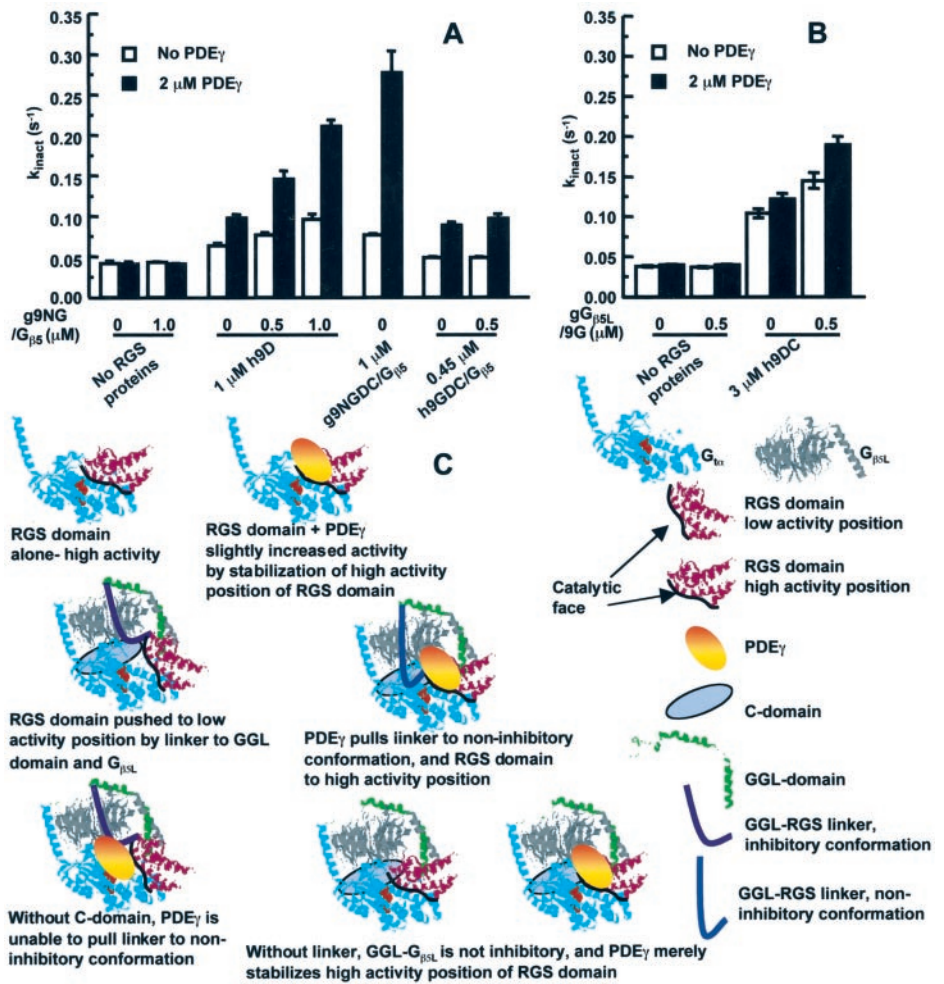


FIG. 7. Direction of PDE_γ effect (enhancement or inhibition) on the GAP activity of RGS members is determined by the RGS domains. Single turnover assays of G_{τα} GTPase with or without PDE_γ. *A*, concentration dependence of the GAP activity of g7NGDC-G_{β5S} and g9NGDC-G_{β5}. In contrast to g9NGDC-G_{β5}, the GAP activity of g7NGDC-G_{β5S} is not stimulated but rather inhibited by PDE_γ. *B*, addition of g9NG-G_{β5} significantly enhances the GAP activity of both h9DC and h7DC but does not change the direction of PDE_γ effect on the GAP activity of h9DC (enhancement) and the GAP activity of h7DC (inhibition).

seems likely that the complexity of this GAP, far greater than that needed for simple constitutive acceleration of G_{τα} GTP hydrolysis, has evolved to provide fine tuning of the kinetics of inactivation. 3) The domains of RGS9-1 external to the catalytic RGS domain contribute to the tight regulation and fine tuning by G_{β5L} and PDE_γ. The GGL domain is required for recruiting G_{β5L}, and these two modules provide most of the regulatory interactions. The C-terminal domain, unique to RGS9-1, is essential for enabling PDE_γ to overcome the inhibition imposed by GGL-G_{β5}, and the N-terminal domain may play a minor role as well.

The conclusion from the present work that RGS9-1 and G_{β5L} require one another for proper structure and function complies well with previous observations. When elution of detergent-solubilized RGS9-1 from various chromatography columns was monitored by specific antibodies, G_{β5L} was found to co-elute (11). RGS9-1 knockout mice (4) contained no detectable G_{β5L} protein, despite the presence of mRNA at normal levels or higher. Likewise, co-precipitation of G_{β5S} with RGS7 antibodies (13, 32) and of RGS7 and RGS6 with G_{β5} antibodies (14) points to obligate heterodimeric (or higher order) complexes for these proteins as well. RGS7 has also been found to require

co-expression of $G_{\beta 5}$ to allow isolation in stable soluble form from baculovirus-infected insect cells (33) or transfected COS-7 cells (32).

Our results also form a coherent picture when compared with the folding and stability requirements of conventional G_{β} subunits. G_{β} translated *in vitro* in the absence of G_{γ} has a less compact structure than $G_{\beta\gamma}$, is unstable, and tends to aggregate (34). $G_{\beta 2}$ and $G_{\gamma 2}$ subunits, when expressed independently in insect cells, could be purified using detergent but did not form an active complex when mixed (35).

Although we cannot say with certainty whether the mutual dependence of RGS9-1 and $G_{\beta 5L}$ *in vivo* is at the level of translation, folding, stabilization against aggregation, and proteolysis or all three, the *in vitro* results imply that both folding and stabilization of each subunit depends on the other.

Reports on the roles of $G_{\beta 5S}$ and $G_{\beta 5L}$ in regulation of GAP activity are somewhat less consistent. In one case, $G_{\beta 5S}$ was described as blocking binding of RGS7 to G_{α} , suggesting that it could block GAP activity (16). However, RGS11 bound to $G_{\beta 5}$ displayed GAP activity toward G_{α} (17), and $G_{\beta 5S}$ co-expression dramatically enhanced the activities of both RGS7 and RGS9-2 in accelerating muscarinic responses of GIRK channels in an oocyte expression system (12). Our results indicate that $G_{\beta 5S}$ and $G_{\beta 5L}$ can either enhance or inhibit GAP activity, depending on additional interactions, such as those with the effector. Thus, the function of $G_{\beta 5S}$ and $G_{\beta 5L}$ appears to be to provide additional constraints on catalytic activity that allow for fine tuning of response kinetics. $G_{\beta 5L}$ and $G_{\beta 5S}$ are also likely involved in discrimination by RGS proteins among G_{α} subunits. The RGS domain of RGS7 efficiently accelerates GTP hydrolysis by either $G_{\alpha 1}$ or $G_{\alpha 2}$ (36), but the RGS7- $G_{\beta 5S}$ complex only works well with $G_{\alpha 2}$ (33).

The results described here do not reveal whether $G_{\beta 5L}$ interacts directly with G_{α} , but if it does the mode of binding during GTPase acceleration must very different from that of $G_{\beta 1}$ binding to G_{α} -GDP, because several key residues of G_{α} involved in $G_{\beta 1}$ interactions are occluded by the RGS domain in the $G_{\beta 1}$ -RGS4 structure (37). In this structure, the C and N termini of the RGS domain were in relatively close proximity, so it may be that the C terminus of RGS9-1 is positioned near or in contact with $G_{\beta 5L}$ -GGL.

The dramatic effects of PDE γ on GAP activity of the RGS9-1- $G_{\beta 5L}$ complex, as compared with its very modest effects on the RGS domain (6), suggest a conformational switch involving $G_{\beta 5L}$, the GGL domain, the RGS domain, the C-terminal domain, and PDE γ . Because the dependence on PDE γ is greatly reduced when the $G_{\beta 5L}$ -GGL complex is not covalently attached to the RGS domain, it seems likely that the connecting peptide chain (25 residues between the positions corresponding to the end of the C-terminal α helix of G_{γ} and the beginning of the N-terminal helix of the RGS domain), imposes an inhibitory constraint that is relieved by PDE γ (Fig. 6C). Thus PDE γ likely affects not the conformational state of the $G_{\beta 5L}$ -GGL itself so much as its position relative to the RGS domain. Because many features of this machinery are conserved in the complexes of $G_{\beta 5S}$ with RGS7, RGS6, RGS11, and likely EGL-10, similar conformational switching mechanisms, involving effectors or other regulatory proteins, may regulate their activities as well. Such mechanisms may help to explain how RGS proteins, ini-

tially thought to be rather promiscuous in their actions, can select not only the G protein-effector pairs on which they should act but also the times at which they should do so.

Acknowledgments—We thank J. Gray, L. Zimmerman, M. Offield, and R. Grainger for advice on transgenesis and F. He for help in expression and purification of proteins from *E. coli*.

REFERENCES

- Koelle, M. R., and Horvitz, H. R. (1996) *Cell* **84**, 115–125
- Berman, D. M., Wilkie, T. M., and Gilman, A. G. (1996) *Cell* **86**, 445–452
- Cowan, C. W., Fariss, R. N., Sokal, I., Palczewski, K., and Wensel, T. G. (1998) *Proc. Natl. Acad. Sci. U. S. A.* **95**, 5351–5356
- Chen, C. K., Burns, M. E., He, W., Wensel, T. G., Baylor, D. A., and Simon, M. I. (2000) *Nature* **403**, 557–560
- McEntaffer, R. L., Natochin, M., and Artemyev, N. O. (1999) *Biochemistry* **38**, 4931–4937
- He, W., Cowan, C. W., and Wensel, T. G. (1998) *Neuron* **20**, 95–102
- Skiba, N. P., Yang, C. S., Huang, T., Bae, H., and Hamm, H. E. (1999) *J. Biol. Chem.* **274**, 8770–8778
- Arshavsky, V. Y., and Bownds, M. D. (1992) *Nature* **357**, 416–417
- Tsang, S. H., Burns, M. E., Calvert, P. D., Gouras, P., Baylor, D. A., Goff, S. P., and Arshavsky, V. Y. (1998) *Science* **282**, 117–121
- Sowa, M. E., He, W., Wensel, T. G., and Lichtarge, O. (2000) *Proc. Natl. Acad. Sci. U. S. A.* **97**, 1483–1488
- Makino, E. R., Handy, J. W., Li, T., and Arshavsky, V. Y. (1999) *Proc. Natl. Acad. Sci. U. S. A.* **96**, 1947–1952
- Kovoor, A., Chen, C. K., He, W., Wensel, T. G., Simon, M. I., and Lester, H. A. (2000) *J. Biol. Chem.* **275**, 3397–3402
- Cabrera, J. L., de Freitas, F., Satpaev, D. K., and Slepak, V. Z. (1998) *Biochem. Cell Biol.* **249**, 898–902
- Zhang, J. H., and Simonds, W. F. (2000) *J. Neurosci.* **20**, RC59
- Snow, B. E., Betts, L., Mangion, J., Sondek, J., and Siderovski, D. P. (1999) *Proc. Natl. Acad. Sci. U. S. A.* **96**, 6489–6494
- Levay, K., Cabrera, J. L., Satpaev, D. K., and Slepak, V. Z. (1999) *Proc. Natl. Acad. Sci. U. S. A.* **96**, 2503–2507
- Snow, B. E., Krumins, A. M., Brothers, G. M., Lee, S. F., Wall, M. A., Chung, S., Mangion, J., Arya, S., Gilman, A. G., and Siderovski, D. P. (1998) *Proc. Natl. Acad. Sci. U. S. A.* **95**, 13307–13312
- Zeng, W., Xu, X., Popov, S., Mukhopadhyay, S., Chidiac, P., Swistok, J., Danho, W., Yagaloff, K. A., Fisher, S. L., Ross, E. M., Muallem, S., and Wilkie, T. M. (1998) *J. Biol. Chem.* **273**, 34687–34690
- Siderovski, D. P., Strockbine, B., and Behe, C. I. (1999) *Crit. Rev. Biochem. Mol. Biol.* **34**, 215–251
- Cowan, C. W., He, W., and Wensel, T. G. (2000) *Prog. Nucleic Acids Res. Mol. Biol.* **65**, 341–359
- Rahman, Z., Gold, S. J., Potenza, M. N., Cowan, C. W., Ni, Y. G., He, W., Wensel, T. G., and Nestler, E. J. (1999) *J. Neurosci.* **19**, 2016–2026
- Zhang, K., Howes, K. A., He, W., Bronson, J. D., Pettenati, M. J., Chen, C., Palczewski, K., Wensel, T. G., and Baehr, W. (1999) *Gene (Amst.)* **240**, 23–34
- Harper, J. W., Adami, G. R., Wei, N., Keyomarsi, K., and Elledge, S. J. (1993) *Cell* **75**, 805–816
- Watson, A. J., Aragay, A. M., Slepak, V. Z., and Simon, M. I. (1996) *J. Biol. Chem.* **271**, 28154–28160
- Fletcher, J. E., Lindorfer, M. A., DeFilippo, J. M., Yasuda, H., Guilford, M., and Garrison, J. C. (1998) *J. Biol. Chem.* **273**, 636–644
- Cowan, C. W., Wensel, T. G., and Arshavsky, V. Y. (2000) *Methods Enzymol.* **315**, 524–538
- Kroll, K. L., and Amaya, E. (1996) *Development* **122**, 3173–3183
- Peng, H. B. (1991) *Methods Cell Biol.* **36**, 657–662
- Nieuwkoop, P. D., and Faber, J. (1967) *Normal Table of Xenopus laevis*, 2nd Ed., Elsevier/North Holland, Amsterdam
- Arshavsky, V. Y., Dumke, C. L., Zhu, Y., Artemyev, N. O., Skiba, N. P., Hamm, H. E., and Bownds, M. D. (1994) *J. Biol. Chem.* **269**, 19882–19887
- Angleson, J. K., and Wensel, T. G. (1993) *Neuron* **11**, 939–949
- Wetherow, D. S., Wang, Q., Levay, K., Cabrera, J. L., Chen, J., Willars, G. B., and Slepak, V. Z. (2000) *J. Biol. Chem.* **275**, 24872–24880
- Posner, B. A., Gilman, A. G., and Harris, B. A. (1999) *J. Biol. Chem.* **274**, 31087–31093
- Schmidt, C. J., and Neer, E. J. (1991) *J. Biol. Chem.* **266**, 4538–4544
- Iniguez-Lluhi, J. A., Simon, M. I., Robishaw, J. D., and Gilman, A. G. (1992) *J. Biol. Chem.* **267**, 23409–23417
- Shuey, D. J., Betty, M., Jones, P.-G., Khawaja, X.-Z., and Cockett, M. I. (1998) *J. Neurochem.* **70**, 1964–1972
- Tesmer, J. J., Berman, D. M., Gilman, A. G., and Sprang, S. R. (1997) *Cell* **89**, 251–261
- Lambright, D. G., Sondek, J., Bohm, A., Skiba, N. P., Hamm, H. E., and Sigler, P. B. (1996) *Nature* **379**, 311–319